ARTICLES

Journal of Semiconductors
(2021) 42, 092802
doi: 10.1088/1674-4926/42/9/092802
JOS

Effect of the post-gate annealing on the gate reliability of AlGaN/GaN HEMTs

Changxi Chen[1, 2], Quan Wang[1, 3], Wei Li[1], Qian Wang[1], Chun Feng[1, 2], Lijuan Jiang[1, 2], Hongling Xiao[1, 2], and Xiaoliang Wang[1, 2, †]

[1]Key Lab of Semiconductor Materials Science, Institute of Semiconductors, Chinese Academy of Sciences, Beijing 100083, China

[2]Center of Materials Science and Optoelectronics Engineering and School of Microelectronics, University of Chinese Academy of Sciences, Beijing 100049, China

[3]State Key Laboratory of Crystal Materials, Shandong University, Jinan 250100, China

Abstract: In this paper, we investigated the effect of post-gate annealing (PGA) on reverse gate leakage and the reverse bias reliability of $Al_{0.23}Ga_{0.77}N$/GaN high electron mobility transistors (HEMTs). We found that the Poole–Frenkel (PF) emission is dominant in the reverse gate leakage current at the low reverse bias region ($V_{th} < V_G < 0$ V) for the unannealed and annealed HEMTs. The emission barrier height of HEMT is increased from 0.139 to 0.256 eV after the PGA process, which results in a reduction of the reverse leakage current by more than one order. Besides, the reverse step stress was conducted to study the gate reliability of both HEMTs. After the stress, the unannealed HEMT shows a higher reverse leakage current due to the permanent damage of the Schottky gate. In contrast, the annealed HEMT shows a little change in reverse leakage current. This indicates that the PGA can reduce the reverse gate leakage and improve the gate reliability.

Key words: AlGaN/GaN HEMTs; gate leakage; PF emission; post-gate annealing (PGA)

Citation: C X Chen, Q Wang, W Li, Q Wang, C Feng, L J Jiang, H L Xiao, and X L Wang, Effect of the post-gate annealing on the gate reliability of AlGaN/GaN HEMTs[J]. *J. Semicond.*, 2021, 42(9), 092802. http://doi.org/10.1088/1674-4926/42/9/092802

1. Introduction

In recent years, AlGaN/GaN high electron mobility transistors (HEMTs) have attracted a lot of attention, owing to their excellent properties for high-power and high-frequency applications[1–3]. In order to guarantee the success in applications of AlGaN/GaN HEMTs, the device reliability is a critical issue to be focused on. Although the quality of material and design of the device has greatly improved over the years, there are still several reliability problems in AlGaN/GaN HEMTs, such as gate degradation, inverse piezoelectric effect and hot electron effect[4–6].

In the off-state biased HEMTs, the inverse piezoelectric effect or gate degradation will appear if the applied bias exceeds the so-called "critical voltage", which is often obtained by performing reverse bias step-stress experiments. The inverse piezoelectric effect and gate degradation are respectively related to the formation of crystallographic defects due to the strain relaxation[5], and the traps generated at the gate/AlGaN interface[7]. Thus, the gate degradation could happen at a relatively low reverse bias compared to the inverse piezoelectric effect. Marcon *et al.*[7] suggested the gate degradation as an electric field accelerated phenomenon, which indicates the leakage current through the metal–semiconductor interface may have a great influence on gate degradation of HEMTs. For this reason, understanding the mechanisms of gate leakage are very helpful to solve the gate degradation issue. Many leakage mechanisms in AlGaN/GaN Schottky contact have been proposed[8–12]. Among these mechanisms, the trap-assisted tunneling (TAT), and Poole–Frenkel (PF) emission through a continuum of trap states related to the conductive dislocation are considered to be the two main leakage mechanisms at a moderate electric field[8–12]. The leakage current may be governed by Fowler–Nordheim (FN) tunneling when the electric field across the AlGaN barrier is strong enough[11]. Many attempts have been made to reduce the gate leakage currents by using gate dielectrics[13], surface treatment[14], and post-gate-annealing (PGA)[15]. In the early reports, the PGA has been proven to be an effective method, which can reduce the gate leakage current and increase the breakdown voltage of GaN-based HEMTs[16]. However, studies on the difference between the gate leakage mechanisms before and after the PGA are always ignored, and the effect of the PGA on the reverse-bias gate reliability have been rarely reported.

In this paper, temperature-dependent current–voltage characteristics were carried out to investigate the reverse leakage mechanism of HEMTs at low reverse gate bias before and after the PGA process. Furthermore, the Schottky gate reliability of the unannealed and annealed HEMTs were studied by the reverse step stress and the reverse gate leakage currents of both HEMTs after the step-stress were compared and analyzed.

2. Experiment

The AlGaN/GaN HEMT structures were grown on a 2-inch sapphire substrate by metal organic chemical vapor deposition (MOCVD). The epitaxial structure consists of a 3 μm GaN

Correspondence to: X L Wang, xlwang@semi.ac.cn
Received 1 APRIL 2021; Revised 16 APRIL 2021.
©2021 Chinese Institute of Electronics

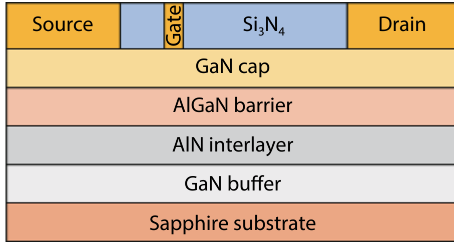

Fig. 1. (Color online) The cross-section schematic of the AlGaN/GaN HEMT.

buffer layer, a 1 nm AlN insertion layer, a 20 nm $Al_{0.23}Ga_{0.77}N$ barrier layer, and a 3 nm GaN cap layer, as shown in Fig. 1. Ohmic metallization Ti/Al/Ti/Au (20/100/40/50 nm) were first deposited, and annealed in a N_2 atmosphere at 870 °C for 30 s. The specific resistivity was 1 × 10^{-5} Ω·cm^2 calculated by the transmission line method (TLM). The devices isolation was conducted by inductively coupled plasma (ICP) dry etching with an etch depth of 180 nm. Ni/Au (40/200 nm) metallization were sputtered and lifted off to form the Schottky gate. Finally, the devices were passivated by a 200 nm thick Si_3N_4 layer deposited by plasma enhanced chemical vapor deposition (PECVD). The gate length, gate width, spacing of gate to drain, and spacing of the gate to source are 3, 100, 20, 5 μm, respectively. To optimize the post-gate-annealing condition, the wafer was cleaved to several pieces after fabrication accomplishment. The annealing temperature was chosen to be 400 °C as referred from the works[17], and the annealing time was varied with 1, 3, 5, and 10 min, respectively. A tradeoff between the gate leakage and output current capacity of HEMTs was considered after the gate annealing, thus the post-gate-annealing condition was selected as 400 °C in N_2 atmosphere for 1 min. Current–voltage (*I*–*V*) curves of gate leakage were measured in the temperature range of 298–458 K and capacitor–voltage (*C*–*V*) measurement was carried out on gate diode at the frequency of 1 MHz[18]. Subsequently, reverse gate bias step-stress was performed on the gate electrode with the drain and source grounded.

3. Results and discussion

To investigate the reverse gate leakage mechanisms of the unannealed and annealed HMETs, the gate *I*–*V* characteristics at different temperatures (from 298 to 458 K with a step of 40 K) of both HEMTs are shown in Fig. 2. The reverse gate leakage currents are dependent both on the bias and temperature at low reverse bias (V_{th} < V_G < 0 V, region I), and become nearly saturated at high reverse bias (V_G < V_{th}, region II). This indicates that the leakage current in region I plays a very significant role in gate reverse leakage. Besides, it is found that the reverse gate leakage currents is reduced significantly after the PGA, as shown in Figs. 2(a) and 2(b).

Since many reverse leakage mechanisms are related to the electric fields across the AlGaN barrier layer[8–12], the electric field across the AlGaN barrier should be calculated for further investigation. The electric field across the AlGaN barrier as a function of gate voltage is estimated by[19],

$$E=\frac{q[\sigma_{\rm p}-n_{\rm s}(V)]}{\varepsilon_0\varepsilon_{\rm r}}, \quad (1)$$

where σ_p is the net polarization charge density at the AlGaN/GaN interface, including the piezoelectric polarization charge and spontaneous polarization charge at the AlGaN/GaN interface, n_s is the two-dimensional electronic gas (2DEG) density at the hetero-structure and ε_r is the relative dielectric constant of the AlGaN barrier. The value of σ_p used in Eq. (1) is set to 1.3 × 10^{13} cm^{-2}[20].

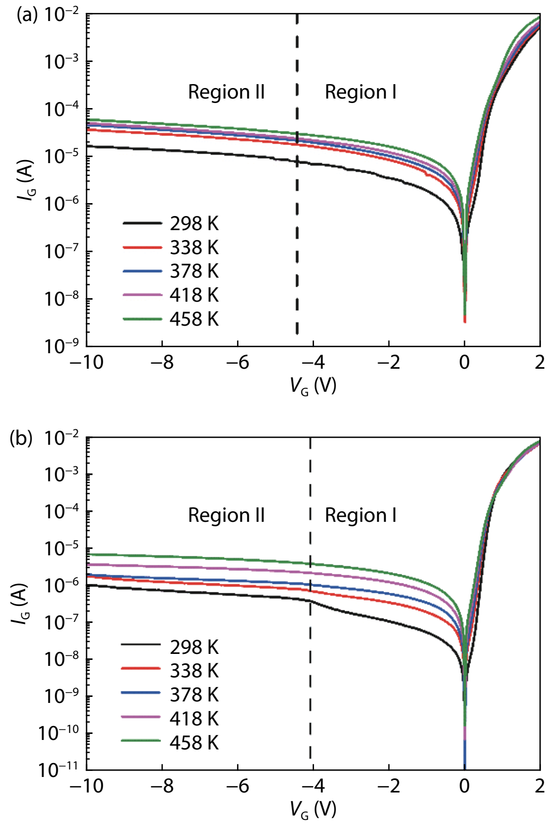

Fig. 2. (Color online) Reverse *I*–*V* characteristics measured from 298 to 458 K in a step of 40 K of (a) unannealed HEMT, (b) annealed HEMT.

The n_s as the function of gate voltage can be calculated by high frequency *C*–*V* measurement. In Fig. 3(a), the gate capacitance versus gate voltage characteristics of both HEMTs are depicted. Subsequently, the corresponding n_s is obtained by integrating the *C*–*V* curve of a gate diode. Thus, the electric fields across AlGaN barriers as the function of gate voltages for both HEMTs are obtained, as shown in Fig. 3(b). At low reverse bias, the electric fields increase with the bias voltages linearly, and become constant when the voltages reach their critical values. The constant electric field comes from the net polarization charges at the AlGaN/GaN interface, due to the total depletion of the 2DEG. In fact, the turning points in Fig. 3(b) represent the threshold voltages of the unannealed and annealed HEMTs, respectively. As can be seen, the threshold voltage of AlGaN/GaN HEMT exhibits a positive shift after the PGA, which can be attributed to the reduction of the electron density under the gate[21].

Because the Poole–Frenkel emission is one of the most common leakage mechanisms at low reverse bias, which is field-dependent as well as temperature-dependent[10]. We first check the validity of PF emission mechanism for the reverse leakage current of AlGaN/GaN HEMTs. Based on the *I*–*V* measurements, the dependence of electric field on gate leakage current for both HEMTs can be determined.

The current density–electric field (*J*–*E*) of PF emission can

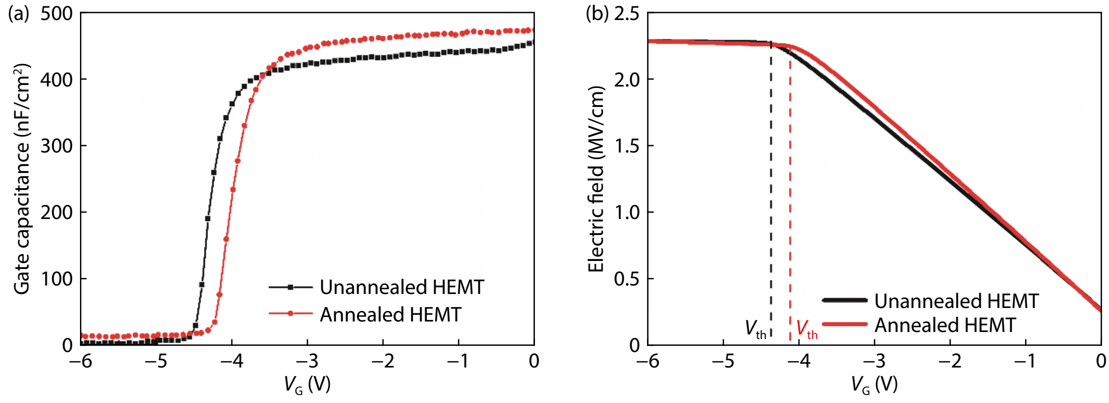

Fig. 3. (Color online) (a) The gate capacitance versus V_G characteristics of both HEMTs. (b) The electric fields across AlGaN as the function of V_G for both HEMTs.

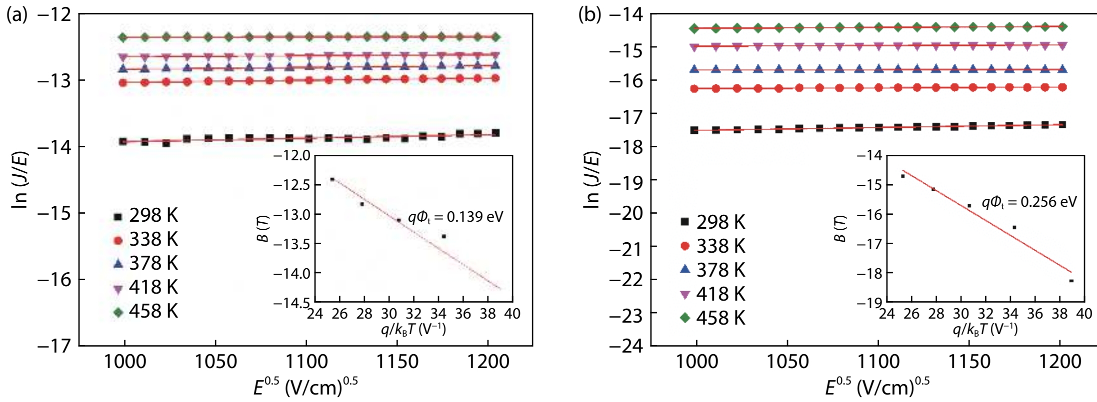

Fig. 4. (Color online) The ln (J/E) versus $E^{0.5}$ and the linear fit for the slope and intercepts of (a) unannealed HEMT, (b) annealed HEMT. Inset: the $B(T)$ versus $\frac{q}{k_BT}$ for the extraction of the height of the trap state.

be expressed by follows[22],

$$J = AE\exp\left[-\frac{\phi_t - \sqrt{q^3E/\pi\varepsilon_0\varepsilon_s(h)}}{k_BT}\right], \tag{2}$$

where A is a constant, ϕ_t is the barrier height for electron emission from trap states to continuum state, k_B is the Boltzmann's constant, T is the temperature, ε_0 is the vacuum dielectric constant and $\varepsilon_s(h)$ is the relative high frequency dielectric constant of the AlGaN barrier[19], q is the electron charge and E is the electric field across the AlGaN barrier. Eq. (2) can be rearranged as

$$\ln\frac{J}{E} = C(T)\sqrt{E} + B(T), \tag{3}$$

where

$$C(T) = \frac{q}{k_BT}\sqrt{\frac{q}{\varepsilon_0\varepsilon_s(h)}}, \tag{4}$$

$$B(T) = \frac{q\phi_t}{k_BT} + \ln m. \tag{5}$$

If the leakage current is dominated by the PF emission at low gate voltage, Eq. (3) points out that $\ln\frac{J}{E}$ should be linearly proportional to $\sqrt{E}$. Indeed, the data points of $\ln\frac{J}{E}$ versus $\sqrt{E}$ in Fig. 4 fit well with the straight line in the temperature range from 298 to 458 K, which provides evidence that the gate leakage mechanisms at low gate voltage of both HEMTs are dominated by the PF emission. From Fig. 4, the y-intercept and slop of $\ln\frac{J}{E}$ versus $\sqrt{E}$ plots can give the values of $B(T)$ and $C(T)$. In the inset of Fig. 4(a), the value of emission barrier height extracted from the slope of plot $B(T)$ versus $\frac{q}{k_BT}$ is 0.139 eV, which is much lower than that of 0.256 eV extracted from the inset of Fig. 4(b). The higher emission barrier of the annealed HEMT is ascribed to the reduction of the electrically active states at the metal/AlGaN interface after the post-gate annealing[23]. This hinders the motion of electrons from the gate to the channel, leading to a reduction of reverse gate leakage current.

In order to study the effects of the PGA on the gate reliability of HEMTs, reverse gate bias step stresses were carried out for the unannealed and annealed HEMTs. As shown in the inset of Fig. 5(a), the gate stress is stepped from –5 to –45 V in a –5 V increment for 60 s per step with the drain and source grounded. In Figs. 5(a) and 5(b), gate leakage current (I_G), source leakage current (I_{GS}) and drain leakage current (I_{GD}) of both devices are displayed, respectively, where the I_G is the sum of I_{GS} and I_{GD}. In Fig. 5(a), three types of the leakage current rise abruptly at different positions, which correspond to the "degradation voltages". The absolute values of the degradation voltage for I_G and I_{GS} are 35 V, which are lower than 40 V for I_{GD}. This suggests that the gate degrada-

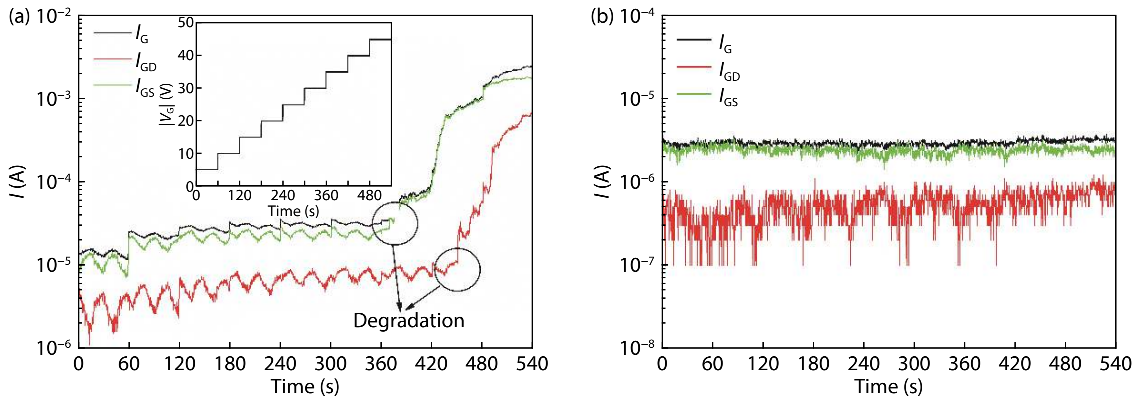

Fig. 5. (Color online) Gate leakage measured during the reverse gate-bias step stress of (a) unannealed HEMT, (b) annealed HEMT. Inset: absolute value of reverse gate-bias step stress versus times (V_{step} = –5 V, t_{step} = 60 s).

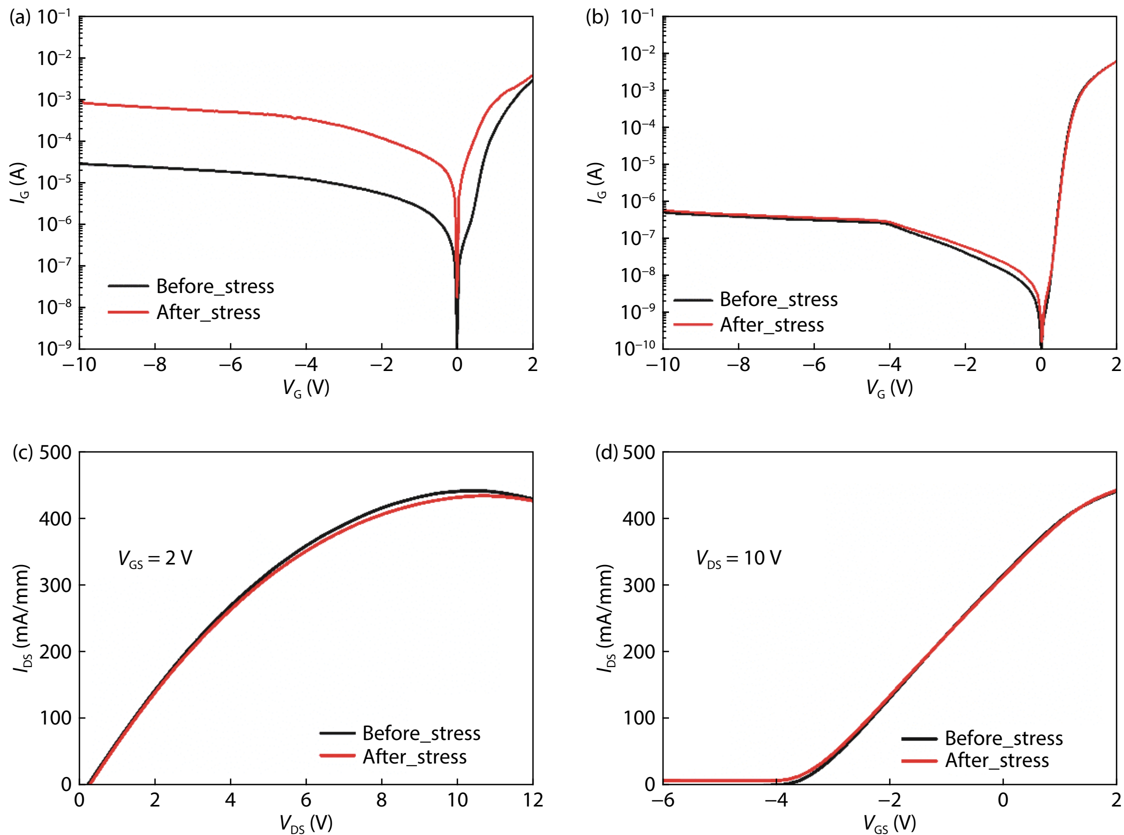

Fig. 6. (Color online) Gate leakage current before and after reverse bias step stress of (a) unannealed HEMT, (b) annealed HEMT, (c) maximum output currents, and (d) transfer characteristics before and after reverse bias step stress of the unannealed HEMT.

tion starts at the source edge near the gate, owing to shorter spacing of the gate to the source. Nevertheless, the gate leakage current of the annealed HEMT increases slowly with the reverse gate voltage, shown in Fig. 5(b), and there is no sharp increase in the three types of currents during the gate stress. The early gate degradation of the unannealed HEMT indicates that the higher initial gate leakage current will accelerate the gate degradation.

For further studying the gate degradation of unannealed and annealed HEMTs, the gate leakage currents before and after reverse step stress for both HEMTs are exhibited in Figs. 6(a) and 6(b). Before the step stress, the reverse gate leakage current of the unannealed HEMT is higher than that of the annealed HEMT, owing to the lower PF emission barrier. After the step stress, the reverse gate leakage current of the unannealed HEMT increases significantly, and it could not recover even waiting for 24 h. Therefore, there must be some new leaking path generated below the gate/AlGaN interface, beneficial for the electrons transporting from the gate to the channel. Conversely, the reverse gate leakage of the annealed HEMT only changes slightly after the gate stress, indicating the improved reliability of the Schottky gate in the annealed HEMT. Additionally, the maximum output currents and the transfer characteristics of the unannealed HEMT before and after the reverse-bias step stress are shown in Figs. 6(c) and 6(d). The maximum output current and the transfer characteristic can almost recover within 5 min after the stress except the leakage current in the pinch-off region. This

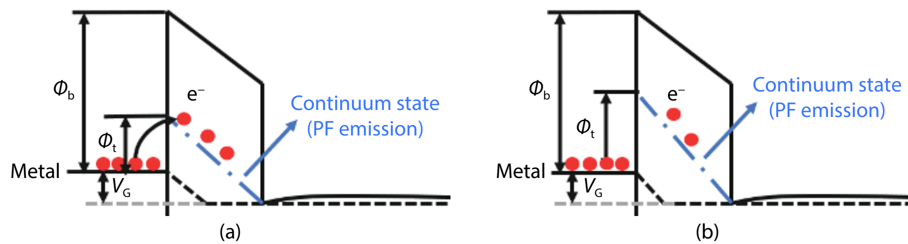

Fig. 7. (Color online) Schematic of the gate leakage at reverse gate bias before the stress of (a) unannealed HEMT, (b) annealed HEMT.

indicates that the permanent gate damage in the unannealed HEMT after the step stress cannot be attributed to the converse piezoelectric effect, which is associated with the creation of macro-defect as reported in Ref. [24].

To better explain the mechanisms of the gate leakage before the reverse step stress for the unannealed and annealed HEMTs, the conduction band diagrams of both HEMTs are depicted in Fig. 7. As labeled by the blue dash-dot line, a continuum of states is presented in the material, which is related to the conductive dislocations in the barrier layer. Electrons can be activated by thermal energy from a trap state to a continuum of states. At low reverse gate bias ($V_{th} < V_G < 0$), the barrier of the emission from the trap state to a continuum of states lowers with the increase of electric field[11]. Hence, the gate leakage current increases with the increase of reverse gate bias. In Fig. 7(a), due to the lower emission barrier of the unannealed HEMT, more electrons can transport from the gate to the channel, resulting in a higher initial gate leakage current. After the step stress, many defects are generated within the AlGaN barrier layer in the unannealed HEMT[25, 26]. As a result, the unannealed HEMT shows a much higher reverse leakage current with the assistance of defects generated after the step stress, as shown in Fig. 6(a). The process of gate leakage before the step stress of the annealed HEMT is also demonstrated in Fig. 7(b). After the PGA, the increased emission barrier in the annealed HEMT hinders the electrons transporting from the gate to the channel, reducing the initial gate leakage current. Therefore, few defects are generated within the AlGaN barrier layer after the step stress in the annealed HEMT, leading to a slight increase of the gate leakage current.

4. Conclusion

In summary, the gate leakage mechanisms at low reverse gate bias and the gate reliability of HEMTs before and after the PGA have been investigated. At the low reverse bias region, the PF emission is dominant in gate leakage of the unannealed and annealed HEMTs. Before the step stress, the gate leakage current is reduced by more than one order in the annealed HEMT, since the emission barrier height is increased from 0.139 to 0.256 eV by the PGA process. In a reverse step-stress experiment, the unannealed HMET exhibits an irreversible degradation at low reverse voltage (V_G = –35 V), indicating the permanent gate degradation. After the gate stress, the gate leakage current of the unannealed HEMT becomes higher, while the gate leakage current of the annealed HEMT remains almost unchanged. The experimental results suggest that the PGA is an effective method to reduce the reverse gate leakage current and improve the reliability of the gate for the AlGaN/GaN HEMTs.

Acknowledgements

This work was supported by the National Key Research and Development Program of China (2017YFB0402900) and the National Natural Sciences Foundation of China (62074144).

References

[1] Wu S, Ma X H, Yang L, et al. A millimeter-wave AlGaN/GaN HEMT fabricated with transitional-recessed-gate technology for high-gain and high-linearity applications. IEEE Electron Device Lett, 2019, 40, 846
[2] Moon J S, Wong J, Grabar B, et al. 360 GHz f_{MAX} graded-channel AlGaN/GaN HEMTs for mmW low-noise applications. IEEE Electron Device Lett, 2020, 41, 1173
[3] Murugapandiyan P, Ravimaran S, William J, et al. Design and analysis of 30 nm T-gate InAlN/GaN HEMT with AlGaN back-barrier for high power microwave applications. Superlattices Microstruct, 2017, 111, 1050
[4] Chen Y Q, Liao X Y, Zeng C, et al. Degradation mechanism of AlGaN/GaN HEMTs during high temperature operation stress. Semicond Sci Technol, 2018, 33, 015019
[5] del Alamo J A, Joh J. GaN HEMT reliability. Microelectron Reliab, 2009, 49, 1200
[6] Gao Z, Rampazzo F, Meneghini M, et al. Degradation mechanism of 0.15 μm AlGaN/GaN HEMTs: Effects of hot electrons. Microelectron Reliab, 2020, 114, 113905
[7] Marcon D, Kauerauf T, Medjdoub F, et al. A comprehensive reliability investigation of the voltage-, temperature- and device geometry-dependence of the gate degradation on state-of-the-art GaN-on-Si HEMTs. 2010 International Electron Devices Meeting, 2010, 20.3.1
[8] Sudharsanan S, Karmalkar S. Modeling of the reverse gate leakage in AlGaN/GaN high electron mobility transistors. J Appl Phys, 2010, 107, 064501
[9] Jos R. Reverse Schottky gate current in AlGaN-GaN high-electron-mobility-transistors. J Appl Phys, 2012, 112, 094508
[10] Zhang H, Miller E J, Yu E T. Analysis of leakage current mechanisms in Schottky contacts to GaN and $Al_{0.25}Ga_{0.75}N$/GaN grown by molecular-beam epitaxy. J Appl Phys, 2006, 99, 023703
[11] Turuvekere S, Rawal D S, DasGupta A, et al. Evidence of Fowler–Nordheim tunneling in gate leakage current of AlGaN/GaN HEMTs at room temperature. IEEE Trans Electron Devices, 2014, 61, 4291
[12] Kotani J, Tajima M, Kasai S, et al. Mechanism of surface conduction in the vicinity of Schottky gates on AlGaN/GaN heterostructures. Appl Phys Lett, 2007, 91, 093501
[13] Zhang S, Liu X Y, Wei K, et al. Suppression of gate leakage current in ka-band AlGaN/GaN HEMT with 5-nm SiN gate dielectric grown by plasma-enhanced ALD. IEEE Trans Electron Devices, 2021, 68, 49
[14] Kim K, Kim T J, Zhang H L, et al. AlGaN/GaN Schottky-gate HEMTs with UV/O_3-treated gate interface. IEEE Electron Device Lett,

2020, 41, 1488
[15] Liu L, Xi Y Y, Ahn S, et al. Characteristics of gate leakage current and breakdown voltage of AlGaN/GaN high electron mobility transistors after postprocess annealing. J Vac Sci Technol B, 2014, 32, 052201
[16] Kim H, Lee J, Liu D M, et al. Gate current leakage and breakdown mechanism in unpassivated AlGaN/GaN high electron mobility transistors by post-gate annealing. Appl Phys Lett, 2005, 86, 143505
[17] Sleptsov E V, Chernykh A V, Chernykh S V, et al. Investigation of the thermal annealing effect on electrical properties of Ni/Au, Ni/Mo/Au and Mo/Au Schottky barriers on AlGaN/GaN heterostructures. J Phys: Conf Ser, 2017, 816, 012039
[18] Visvkarma A K, Laishram R, Kapoor S, et al. Improvement in DC and pulse characteristics of AlGaN/GaN HEMT by employing dual metal gate structure. Semicond Sci Technol, 2019, 34, 105013
[19] Yan D W, Lu H, Cao D S, et al. On the reverse gate leakage current of AlGaN/GaN high electron mobility transistors. Appl Phys Lett, 2010, 97, 153503
[20] Hao M L, Wang Q, Jiang L J, et al. Gate leakage and breakdown characteristics of AlGaN/GaN high-electron-mobility transistors with Fe delta-doped buffer. Nanosci Nanotechnol Lett, 2018, 10, 185
[21] Lin Z J, Kim H, Lee J, et al. Thermal stability of Schottky contacts on strained AlGaN/GaN heterostructures. Appl Phys Lett, 2004, 84, 1585
[22] Turuvekere S, Karumuri N, Rahman A A, et al. Gate leakage mechanisms In AlGaN/GaN and AlInN/GaN HEMTs: Comparison and modeling. IEEE Trans Electron Devices, 2013, 60, 3157
[23] Kim H, Schuette M L, Lee J, et al. Passivation of surface and interface states in AlGaN/GaN HEMT structures by annealing. J Electron Mater, 2007, 36, 1149
[24] Marcon D, Viaene J, Favia P, et al. Reliability of AlGaN/GaN HEMTs: Permanent leakage current increase and output current drop. Proceedings of the 20th IEEE International Symposium on the Physical and Failure Analysis of Integrated Circuits (IPFA), 2013, 249
[25] Chang C Y, Douglas E A, Kim J, et al. Electric-field-driven degradation in off-state step-stressed AlGaN/GaN high-electron mobility transistors. IEEE Trans Device Mater Reliab, 2011, 11, 187
[26] Meneghini M, Stocco A, Bertin M, et al. Time-dependent degradation of AlGaN/GaN high electron mobility transistors under reverse bias. Appl Phys Lett, 2012, 100, 033505

Changxi Chen received his BS degree in Optoelectronics Science and Technology from ShenZhen University, Shenzhen, China, in 2014. He is currently pursuing the Ph.D. degree with the School of Materials Science and Optoelectronic Technology from Institute of Semiconductors, Chinese Academy of Sciences, Beijing, China. His current research interests focus on III–V compound semiconductor materials and devices.

Xiaoliang Wang is a professor and Ph.D. supervisor in the Institute of Semiconductor, Chinese Academy of Sciences. He received his B.S. and M.S. degrees from Northwestern University, Xi'an, China, in 1984 and 1990, respectively, and the Ph.D. degree from the Xi'an Institute of Optics and Precision Mechanics, Chinese Academy of Sciences, Xi'an, and the Institute of Semiconductors, Chinese Academy of Sciences, Beijing, China. His current research interests include III–V compound semiconductor materials and devices. His particular interest has been in the growth and characterization of GaN-based heterostructures and design and fabrication of high power devices. He has published more than 100 articles.